Asian Journal of Pharmaceutical Sciences 13 (2018) 518–526

Available online at www.sciencedirect.com

ScienceDirect

journal homepage: www.elsevier.com/locate/AJPS

Original Research Paper

Enhanced transdermal delivery of meloxicam by nanocrystals: Preparation, *in vitro* and *in vivo* evaluation

Qin Yu[a], Xiying Wu[a], Quangang Zhu[a], Wei Wu[a,b], Zhongjian Chen[a,*], Ye Li[c,**], Yi Lu[a,b,***]

[a] Shanghai Dermatology Hospital, Shanghai 200443, China
[b] Department of Pharmaceutics, School of Pharmacy, Fudan University, Shanghai 201203, China
[c] Shaanxi Academy of Traditional Chinese Medicine, Xi'an 710003, China

ARTICLE INFO

Article history:
Received 19 June 2017
Revised 5 September 2017
Accepted 10 October 2017
Available online 7 December 2017

Keywords:
Meloxicam
Nanocrystals
Transdermal delivery
Nanoprecipitation
Acid-base neutralization

ABSTRACT

Meloxicam (MLX) is efficient in relieving pain and inflammatory symptoms, which, however, is limited by the poor solubility and gastrointestinal side effects. The objective of this study is to develop a nanocrystal formulation to enhance transdermal delivery of MLX. MLX nanocrystals were successfully prepared by the nanoprecipitation technique based on acid-base neutralization. With poloxamer 407 and Tween 80 (80/20, w/w) as mixed stabilizers, MLX nanocrystals with particle size of 175 nm were obtained. The crystalline structure of MLX nanocrystals was confirmed by both differential scanning calorimetry and X-ray powder diffractometry. However, the nanoprecipitation process reduced the crystallinity of MLX. Nanocrystals increased both *in vitro* and *in vivo* transdermal permeation of MLX compared with the solution and suspension counterparts. Due to the enhanced apparent solubility and dissolution as well as the facilitated hair follicular penetration, nanocrystals present a high and prolonged plasma MLX concentration. And 2.58- and 4.4-fold increase in $AUC_{0\rightarrow 24h}$ was achieved by nanocrystals comparing with solution and suspension, respectively. In conclusion, nanocrystal is advantageous for transdermal delivery of MLX.

© 2017 Shenyang Pharmaceutical University. Published by Elsevier B.V.
This is an open access article under the CC BY-NC-ND license.
(http://creativecommons.org/licenses/by-nc-nd/4.0/)

* Corresponding author. Shanghai Dermatology Hospital, 1278 Baode Road, Shanghai 200443,China. Tel.: +86 21 61833007.
** Corresponding author. Shaanxi Academy of Traditional Chinese Medicine, 2 Xihuamen, Xi'an 710003, China. Tel.: +86 29 87251837.
*** Corresponding author. Fudan University, 826 Zhangheng Road, Shanghai 201203, China. Tel.: +86 21 51980084.
E-mail addresses: aajian818@163.com (Z. Chen), liyelsj@163.com (Y. Li), fd_luyi@fudan.edu.cn (Y. Lu).
Peer review under responsibility of Shenyang Pharmaceutical University.

https://doi.org/10.1016/j.ajps.2017.10.004
1818-0876/© 2017 Shenyang Pharmaceutical University. Published by Elsevier B.V. This is an open access article under the CC BY-NC-ND license. (http://creativecommons.org/licenses/by-nc-nd/4.0/)

1. Introduction

Meloxicam (MLX), a highly potent non-steroidal anti-inflammatory drug (NSAID), can inhibit cyclooxygenase activity and block the synthesis of prostaglandins. In clinic, MLX is efficient in relieving pain and inflammatory symptoms in joint diseases such as rheumatoid arthritis and osteoarthritis [1]. Due to the low toxicity, MLX is a good alternative for patients that cannot tolerate other NSAIDs. Nonetheless, the poor solubility and gastrointestinal side effects, including bellyache, dyspepsia, ulceration and bleeding, greatly limit the clinical application of MLX [2]. Transdermal delivery provides an optimal route for MLX to bypass the gastrointestinal adverse effects. In addition, MLX displays distinctive characteristics suitable for transdermal delivery, such as low dose, relatively low molecular weight (354.1), moderate lipophilicity (logP = 1.91 at pH 5.0), and excellent dermal tolerability [3]. However, the poor water-solubility of MLX presents as a hurdle to efficient transdermal delivery. Various approaches employing penetration enhancers [4], lipid vesicles [5] and microemulsions [6] have been adopted to improve the transdermal delivery of MLX.

Nanocrystals are drug crystals with a size generally less than 1 μm [7]. Size reduction to nanometer range significantly increases the apparent solubility and dissolution rates due to the enormously increased specific surface. Therefore, nanocrystals were initially invented to improve the oral bioavailability of poorly soluble drugs [8–10]. Recently, nanocrystals found new applications in transdermal drug delivery [11–13]. The first successful marketing of a rutin nanocrystal product (Juvedical®) in cosmetic market greatly encourages research and development of pharmaceutical transdermal products [10]. The proposed mechanisms for enhanced transdermal permeation by nanocrystals include: i) increased concentration gradient between the formulation and the skin surface due to increased apparent solubility and dissolution; ii) maintenance of the concentration gradient due to increased adhesion with the skin surface; and iii) enhanced hair follicular accumulation, acting as a depot for prolonged release [10,11]. It is hypothesized that transdermal delivery of MLX might be significantly enhanced by the nanocrystal technique. To our best knowledge, transdermal delivery of MLX by nanocrystals has not been investigated yet.

In this study, MLX nanocrystals were prepared by nanoprecipitation based on acid-base neutralization [14–16] and characterized by dynamic light scattering (DLS), scanning electron microscopy (SEM), differential scanning calorimetry (DSC) and X-ray powder diffractometry (PXRD). In addition, both *in vitro* and *in vivo* transdermal penetration were performed to evaluate the enhanced transdermal delivery of MLX by nanocrystals.

2. Materials and methods

2.1. Materials

MLX was purchased from Wanqing Pharmaceutical Co. Ltd. (Suzhou, China), and piroxicam was obtained from Dalian Meilun Biotech Co., Ltd. (Dalian, China). Poloxamer 407 was gifted from BASF-SE. (Germany). Sodium hydroxide, hydrochloric acid, Tween 80 and ammonium acetate were purchased from Sinopharm Chemical Reagent Co., Ltd. (Shanghai, China). Deionized water was prepared by a Milli-Q water purifying system. (Millipore, USA). All other reagents were of analytical grade.

2.2. Preparation of MLX nanocrystals

MLX nanocrystals were prepared following previously established nanoprecipitation technique with modifications [14–16]. In brief, MLX and stabilizers were firstly solubilized in 20 ml NaOH aqueous solution (0.05 M), and then 2 ml HCl aqueous solution (0.5 M) was poured into the solution under high speed shearing (T18, IKA, Germany). The high speed shearing continued for several minutes. Single-factor screening was used to optimize the formulation. With particle size as the indicator, the type and the concentration of the stabilizers, as well as the speed and time of high speed shearing were optimized.

Besides, the optimized nanocrystal suspensions were lyophilized by a freeze dryer (Freeze zone 6, Labconco Co., Ltd., KS, USA) for characterization such as PXRD and DSC. In the process, the suspensions were filled in 10 ml vials (2 cm height), and then frozen at −80 °C over 4 h. After that, the frozen samples were lyophilized successively at −40 °C for 24 h (0.02 bar), −20 °C for 24 h (0.02 bar) and 10 °C for 12 h [16].

In addition, MLX suspension and solution were prepared and set as control. MLX suspension was directly prepared by suspending the raw MLX crystals in the stabilizers solution, containing 0.1% (w/v) poloxamer 407/Tween 80 (80/20), under magnetic stirring (RCT basic, IKA, Germany). The average size of the suspension was about 10.3 μm measured by Malvern Zetasizer 3000 Instruments (Malvern, UK). MLX solution was obtained by solubilizing MLX in the stabilizer aqueous solution, containing 0.1% (w/v) poloxamer 407/Tween 80 (80/20). In order to solubilize MLX, PEG 400 was added to the solution to a concentration of 20% (v/v) and the pH of the solution was adjusted to pH 8 with sodium hydroxide solution (1 M) [17]. All formulations have equal concentrations of MLX and stabilizers, respectively.

2.3. Measurement of MLX

MLX was measured by HPLC on an Agilent 1260 HPLC system (Agilent, USA) with an ultraviolet detector set at wavelength of 355 nm, a column heater set at 30 °C, and an automatic injector with injection volume of 20 μl. The mobile phase consisted of 55% methanol and 45% ammonium acetate aqueous solution (0.1 mol/l) [2]. MLX was separated by a C_{18} column (Eclipse XDB-C18 column, 4.6 mm × 150 mm, 5 μm; Agilent, USA). The retention time was about 5.5 min. Both *in vitro* and *in vivo* MLX samples were detected under these conditions. The MLX concentration (C) is linear with its peak area (A) for measuring *in vitro* penetration samples in the range of 0.04 to 10.2 μg/ml with a typical calibration curve of $C = 0.0118A + 0.0481$, $r^2 = 0.9999$. Accuracy of the measurement is 100.80% ± 0.99%. Intra- and inter-day precision were all below 2%.

2.4. *In vitro characterization*

2.4.1. *Particle size*

Malvern Zetasizer Nano® Instruments (Malvern, UK) was used to measure the average particle size of MLX nanocrystals. It was equipped with a 4 mW He-Ne laser (633 nm) at 25 °C based on photon correlation spectroscopy. Samples were directly measured without dilution. The results were analyzed by the Zetasizer Software provided by Malvern Instruments. Each sample was measured in triplicate.

2.4.2. *Morphology*

The morphology of MLX raw material and nanocrystals were observed by SEM (QuantaTM 250, FEI, USA). The samples were directly fixed onto the aluminum stub using double-sided tape. The samples were then sputter coated with a conductive layer of gold palladium and observed at an accelerating excitation voltage of 10 kV.

2.4.3. *DSC*

A 204A/G Phoenix® DSC instrument (Zetzsch, Selb, Baveria, Germany) was used to assess the thermal behavior of samples: MLX raw material, poloxamer 407, physical mixture and nanocrystals. Samples were sealed in aluminum pan and heated at 5 °C/min from 25 to 320 °C in the atmosphere of nitrogen.

2.4.4. *PXRD*

A D8 ADVANCE X-ray diffractometer (Bruker, Germany) was utilized to perform PXRD test, and a copper radiation source was used as the anode material. MLX raw material, poloxamer 407, NaCI, physical mixture and nanocrystals were scanned from 5° to 50° 2θ range at a scan rate of 4°/min with a step angle of 0.02° and counting time of 1 s/step.

2.5. *In vitro transdermal permeation*

In vitro transdermal permeation of MLX nanocrystals was evaluated using a vertical Franz diffusion cell, providing a diffusion area of 3.21 cm^2 and a receptor volume of 8.45 ml. MLX solution and suspensions were set as control groups. Abdominal skin of Sprague Dawley rats was adopted as skin model. Each group was parallel measured in six skin samples. All animal experiments were approved by the institutional ethical committee and performed in compliance with the institutional guidelines at School of Pharmacy, Fudan University. One day prior to the experiment, the abdominal hair was cut firstly by an electric hair clipper (FLYCO, Shanghai, China) and then removed thoroughly by depilatory reagent (Veet, France). Just before the experiments, the rats were sacrificed and the skin was carefully excised; the subcutaneous fat and muscle tissues were removed with tweezers; then the skin was washed with PBS solution (pH 7.4) [18]. The excised skin was mounted between the donor and the receptor chambers of the Franz diffusion cell with dermis contacting with the receptor medium and the stratum corneum facing upward the donor chamber. Then, 500 µl formulations (equivalent to 2.25 mg MLX) were applied onto the surface of the skin through the opening of the donor chamber. The receptor chamber was filled with PBS (pH 7.4) containing 20% (v/v) PEG 400 to maintain the sink condition [19], which was stirred at 160 rpm. The temperature of the receptor medium was maintained at 32 ± 0.5 °C. At predetermined time intervals (1, 2, 4, 6, 8, 10, 12, and 24 h), 2 ml samples were withdrawn and replaced with fresh receptor medium at equal temperature. Each sample was centrifuged at 8000 rpm for 10 min, supernatant was diluted to a suitable concentration for HPLC detection.

After 24 h of *in vitro* transdermal penetration, the drug residual in the skin was measured according to literature [20]. Briefly, the skin was washed with PBS solution (pH 7.4) and subjected to tape striping for once to remove MLX formulation that may adhere onto the surface of the skin. Then the skin was blotted dry with a soft tissue. The skin was weighed and cut into pieces, into which, 50 µl piroxicam (internal standard) methanol solution (100.6 µg/ml) and 5 ml methanol were added. MLX was extracted under ultrasonication lasting 45 min. The mixture was then separated by centrifugation at 8000 rpm for 10 min. The organic supernatant was separated and dried under nitrogen flow at 40 °C. The residue was dissolved by mobile phase and analyzed by HPLC. The chromatographic conditions are the same with that used in the measurement of *in vitro* permeation samples. The peak area ratio *R* of MLX to the internal standard was recorded for measurement. Within the range of 0.04 to10.2 µg/ml, good linearity was obtained for measuring the dermal residue of MLX. A typical calibration curve was $C = 0.457R\text{-}0.0121$, $r^2 = 0.9998$. Accuracy of the measurement was 99.43 ± 1.32%. Intra- and inter-day precisions all met the analytical method requirements.

The cumulative permeation amount of MLX (Q_t) was calculated as follows [21].

$$Q_t = V_r C_t + \sum_{i=0}^{t-1} V_s C_i$$

where C_t and C_i are the MLX concentrations in the receiver solution at each time point and in the ith withdrawn sample solution, respectively, while V_r and V_s are the volumes of the receiver solution and the sample, respectively.

The cumulative permeation amount per unit skin area (Q_t/S) versus time curve was drawn. MLX steady state flux (J_{ss}) across the skin was the slope of the linear portion of the curve. Drug deposition per unit skin area (Q_r) was calculated through dividing the amount of MLX residual in the skin (Q) by the effective skin area for permeation (S).

2.6. *In vivo transdermal delivery*

The *in vivo* transdermal delivery was performed in Sprague Dawley rats (Male, 170–180 g) with MLX solution and suspension as control. The animals were divided into 3 groups, each containing 48 rats. One day prior to the experiment, the abdominal hair of the rats were removed just like *in vitro* penetration study. The rats were fasted overnight but had free access to water before drug administration. For ease of drug administration, the donor cell with diffusion area of 0.77 cm^2 was fixed, with super glue, on the abdominal surface of the anaesthetized rats by intraperitoneal injection of 10% chloral hydrate aqueous solution. Then the rats were fixed by rat fixators. Three formulations, MLX nanocrystals, solution

and suspensions, 100 µl (equivalent to 0.45 mg MLX), were applied to the skin surface through the donor cell, respectively. At predetermined time intervals (1, 2, 3, 4, 6, 8, 12 and 24 h), blood samples (1.0 ml) were withdrawn through the orbital vein into the heparinized tubes, and centrifuged at 6000 rpm for 5 min. The plasma was transferred into 1.5 ml tubes. In the meantime, the rats were sacrificed. The effective abdominal skin was carefully excised to measure the drug residual. The plasma and the skin samples were kept frozen at −20 °C till analysis.

The drug residual in the skin was measured just like *in vitro* penetration study. Liquid–liquid extraction method was used to extract MLX in the plasma [22]. Briefly, 10 µl piroxicam methanol solution (10.06 µg/ml) and 40 µl HCl (5 M) were added to 200 µl plasma sample. After vortex-mixing for 30 s, 2 ml diethyl ether was added and vortex-mixing was continued for another 10 min to extract MLX. After centrifugation at 5000 rpm for 3 min, the organic layer was transferred to a new tube and evaporated under nitrogen flow at 40 °C. The residue was reconstituted with 100 µl mobile phase and analyzed by HPLC. Within the range of 0.02 to 5.1 µg/ml, MLX concentration showed good linear relationship with *R*, with a typical calibration curve $C = 0.3300R + 0.0001$, $r^2 = 0.9996$. Accuracy of the measurement was 98.54 ± 2.20%. Intra- and inter-day precisions all met the analytical method requirements.

Pharmacokinetic analysis was performed by a model independent method. C_{max} and T_{max} were observed as raw data. Area under the curve (plasma MLX concentration versus time) to the last measured point 24 h ($AUC_{0\rightarrow 24h}$) was calculated according to the linear trapezoidal rule.

2.7. Statistical analysis

Raw data were analyzed with SPSS statistical software (version 11.0, SPSS, Inc., Chicago, IL, USA). In order to determine the significance of differences between groups, post-hoc multiple comparisons were performed with one-way ANOVA and Student–Newman–Keuls test (q test). *P* value less than 0.05 was considered statistically significant.

3. Results and discussion

3.1. Preparation of MLX nanocrystals

MLX nanocrystals have been prepared by top-down technique, more specifically the wet milling process to comminute coarse MLX crystals to nanometer dimension, with purpose to improve the oral bioavailability [23]. Albeit universal to all poorly soluble drugs, this technique suffers from time and energy consuming as well as contamination from erosion of milling media [8,9]. On the contrary, bottom-up techniques grow nanocrystals from drug solution, usually based on antisolvent precipitation of dissolved drugs [8,9]. Although the bottom-up technique is comparatively simple and superior in controlling particle size distribution than the top-down technique, organic solvent is generally required to dissolve drugs, inevitably leading to issues of environmental pollution and labor protection [14]. Therefore, our group introduced a novel nanoprecipitation technique based on acid-base neutralization to prepare nanocrystals of weakly acidic or basic hydrophobic drugs [14]. In these processes, drugs are dissolved in acidic or basic solutions, whereas nucleation was triggered by neutralization under agitation to form nanocrystals. MLX gets pKa values in the range of 4.36 to 4.85 depending on the solution composition [24]. And MLX is suitable to this technique due to the pH dependent solubility, which is 0.012 mg/ml in water, while 0.086×10^{-2} mg/ml in 0.1 M hydrochloride HCl solution [3]. Thus, MLX can be solubilized in alkaline solution and precipitated by neutralization using equal mole HCl solution to grow nanocrystals.

MLX nanocrystals were prepared successfully by nanoprecipitation based on acid-base neutralization with good reproducibility. Since particle size plays an important role in the *in vitro* and *in vivo* performance of nanocrystals, the preparation was optimized with particle size as evaluation index. Fig. 1A shows the effects of different stabilizers on the particle size of MLX nanocrystals. Poloxamer 188, PEG 6000 and SDS cannot provide enough stabilizing effects, producing nanocrystals larger than 1000 nm. On the contrary, Tween 80, poloxamer 407 and HPMC E3 show good controls on the particle size, and nanocrystals smaller than 300 nm were prepared. In addition, poloxamer 407 and Tween 80 are superior to HPMC E3 concerning maintenance of the particle size during storage at 4 °C for 24 h (Fig. 1B). The size of nanocrystals stabilized by HPMC E3 was increased by more than tenfold during storage, while nanocrystals stabilized by poloxamer 407 or Tween 80 were comparatively stable. Nonetheless, the mixed stabilizers of poloxamer 407 and Tween 80, irrespective of the weight ratios, provide better stabilizing effects than the individual ones (Fig. 1C). Then poloxamer 407/Tween 80 (80/20, w/w) were adopted as the mixed stabilizers. Besides the type of the stabilizers, the concentration of the mixed stabilizers was optimized. It was found that the stabilizers concentration significantly influences the particle size of MLX nanocrystals (Fig. 1D). With the concentration decreased from 0.5% to 0.1%, the particle size was slightly increased without significant variation. However, once the concentration was decreased less than 0.1%, the particle size was significantly increased to around 2000 nm. Thus, the stabilizers concentration was set to 0.1%. Similarly, MLX concentration affects the particle size (Fig. 2). When MLX concentration was less than 0.5% (w/v), nanocrystals smaller than 200 nm can be prepared. But once MLX concentration exceeds 0.5%, the particle size was instantly increased to 1000 nm. This might be ascribed to the inadequate stabilizers that absorbed on the surface of the nanocrystals. Therefore, MLX concentration was set to 0.5%. Besides the formula, preparation technique may affect the particle size of the nanocrystals. Speed of high speed shearing had significant influence on particle size of nanocrystals, when the speed of high speed shearing was increased from 9000 to 12000 rpm, particle size increased from 175 nm to 490 nm (Fig. 3A). But extending the shearing time from 1 to 5 min showed no significant influence on particle size (Fig. 3B).

Taking together all the results of single-factor screening, the optimal preparation process of MLX nanocrystals is as follows: MLX (0.5%, w/v) and mixed stabilizers (0.1%, w/v, weight ratio of poloxamer 407/Tween 80 = 80/20) were firstly solubi-

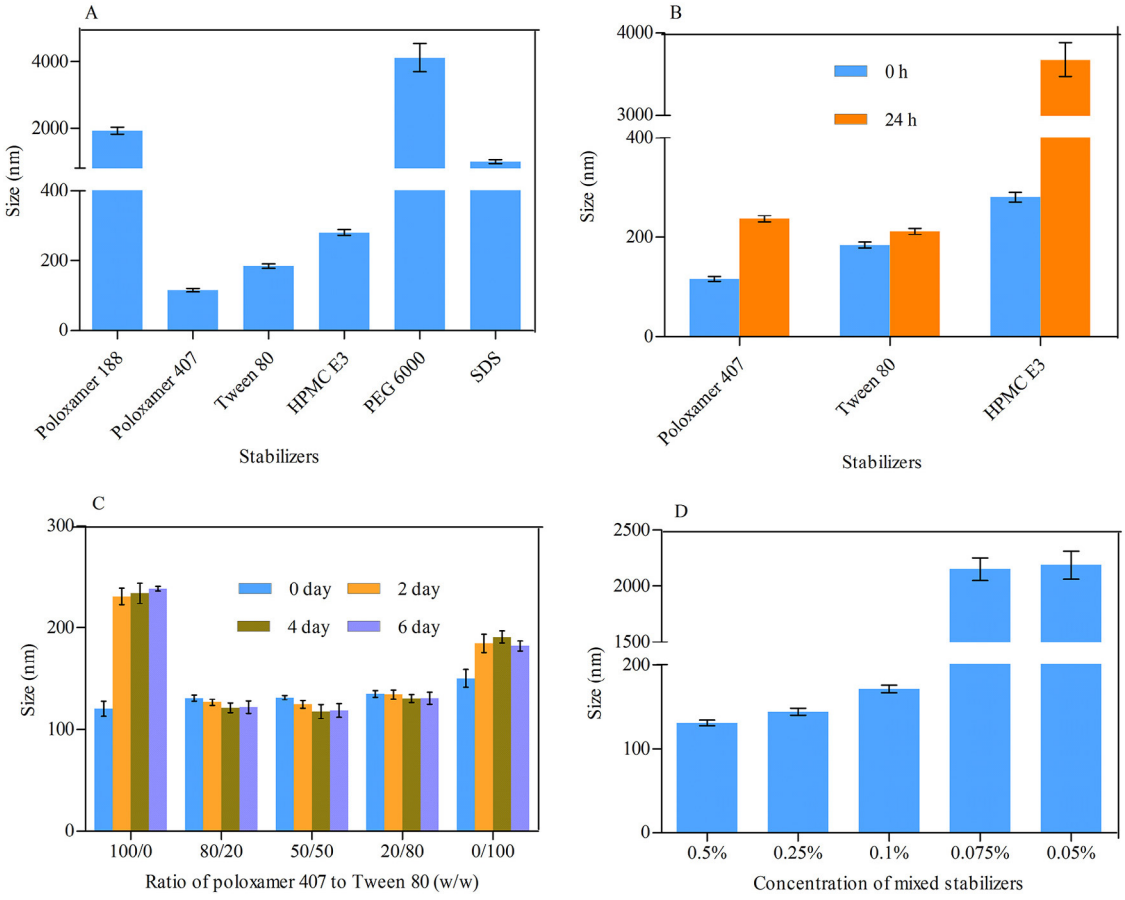

Fig. 1 – (A) Effects of the types of stabilizer on particle size of MLX nanocrystals. (B) Particle size variation during storage at 4 °C from nanocrystals prepared with different types of stabilizers. Effects of (C) weight ratios of poloxamer 407/Tween 80 and (D) concentration of the mixed stabilizers on particle size of MLX nanocrystals.

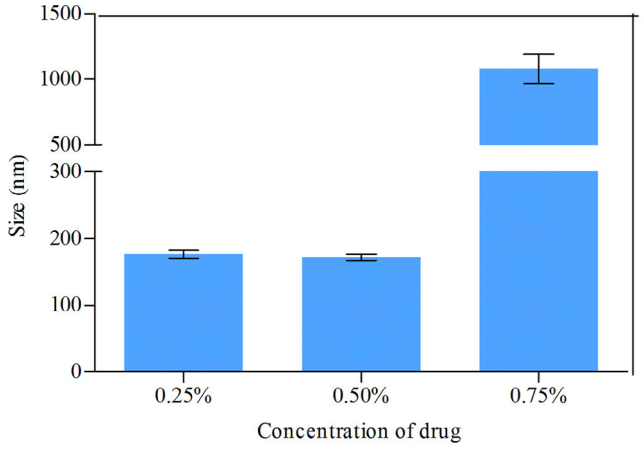

Fig. 2 – Effects of MLX concentration on the particle size of nanocrystals.

lized in 20 ml NaOH aqueous solution (0.05 M), and then 2 ml HCl aqueous solution (0.5 M) was poured into the solution under high speed shearing at 9000 rpm, while the shearing continued for 3 min.

3.2. *Particle size*

The prepared MLX nanocrystals present a mean particle size of 175 ± 4 nm with polydispersity index (PDI) value of 0.167 ± 0.030 (Fig. 4). The particle size and distribution were slightly increased for re-dispersed nanocrystals after lyophilization with mean particle size of 195 ± 5 nm and PDI value of 0.146 ± 0.028 (Fig. 4). The alteration is mainly ascribed to Ostwald ripening and agglomeration of nanosuspensions during lyophilization [25].

3.3. *Morphology*

SEM images of MLX raw material and nanocrystals are shown in Fig. 5 . The observed size is generally in accordance with the measured one by Malvern Zetasizer. MLX raw material presents as rectangular blocks with smooth surfaces. However, the nanocrystals are irregular massive. And the surfaces of the nanocrystals are likely coated by a film, which is mainly ascribed to the adsorption of stabilizers [16]. Coating of stabilizers molecules onto the surfaces of nanocrystals can not only prevent aggregation due to the steric hindrance, but also act as a penetration enhancer to enhance transdermal delivery [26].

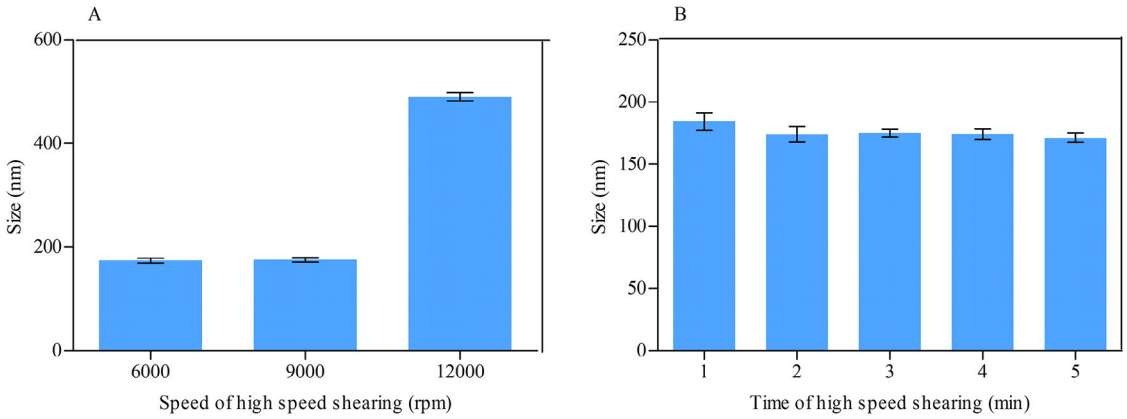

Fig. 3 – Effects of (A) speed and (B) time of high speed shearing on the particle size of MLX nanocrystals.

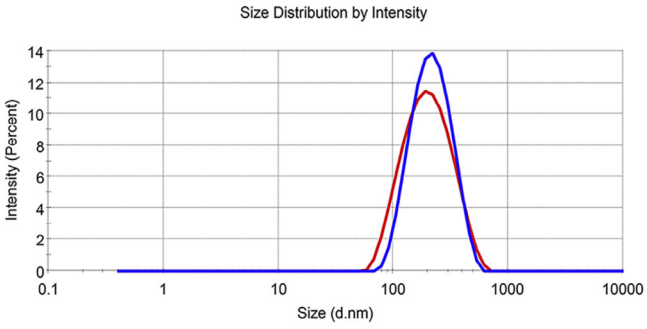

Fig. 4 – Intensity distribution of MLX nanocrystals before (red) and after (blue) lyophylization.

3.4. DSC

DSC thermograms of MLX raw material, poloxamer 407, physical mixture and nanocrystals are depicted in Fig. 6. Raw MLX and poloxamer 407 exhibit endothermic peaks at about 259 °C and 58 °C, respectively, corresponding to their melting points (Fig. 6D and C). These characteristic peaks of MLX and poloxamer are also observed in the thermogram of the physical mixture (Fig. 6B) and nanocrystals (Fig. 6A), revealing crystalline structure of the nanocrystals. However, the endothermic peak of MLX from nanocrystals is broadened as well as 19 °C and 14 °C lower than that from the raw material and the physical mixture, respectively. The broaden endothermic curve as well as the lowered endothermic peak are generally ascribed to the decreased crystallinity upon nanosizing process which was also found in diosmin nanocrystals [27]. But still, the crystallinity of MLX was maintained in nanocrystals, which was further confirmed via PXRD.

3.5. PXRD

The PXRD diagrams of MLX raw material, physical mixture, nanocrystals, NaCl and poloxamer 407 are shown in Fig. 7. The PXRD of NaCl is detected because NaCl is the byproduct of acid-base neutralization in the preparation of nanocrystals. The raw MLX exhibits intense crystalline peaks within 2θ ranges from 10 to 30° with characteristic peaks at 13.06°, 14.98°, 18.59° and 25.84° (Fig. 7A). The diffraction pattern of poloxamer 407 is characterized by peaks around 19.22° and 23.41° (Fig. 7E), while NaCl presents characteristic peaks of 31.76° and 45.63° (Fig. 7D). The diffractogram of the physical mixture is the superposition of its own constituents (Fig. 7B). Characteristic peaks of MLX and poloxamer in the diffractogram of nanocrystals were also observed, revealing crystalline structure (Fig. 7C and inset). However, the intensity of the characteristic MLX peaks from nanocrystals is decreased compared with that from physical mixture, indicating the reduction of the crystallinity of the drug during the process.

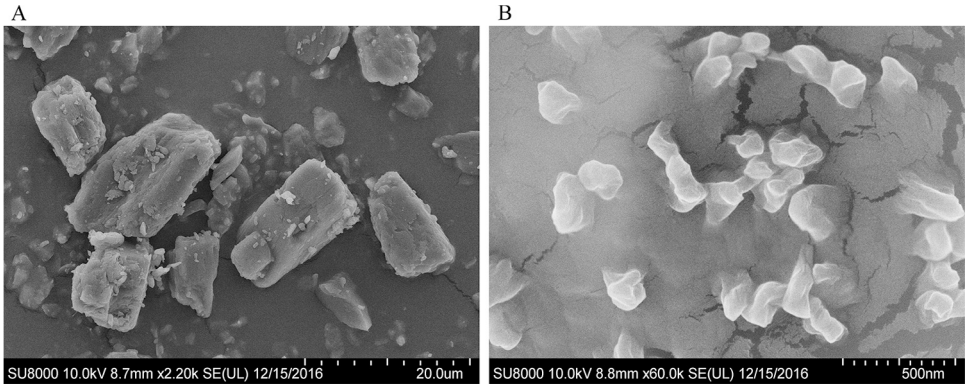

Fig. 5 – SEM photographs of (A) MLX raw material and (B) nanocrystals.

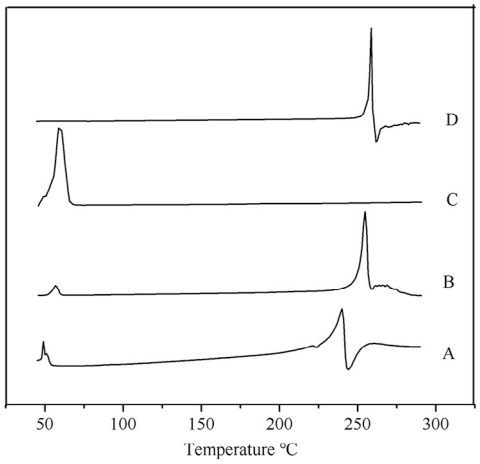

Fig. 6 – DSC thermograms of (A) MLX nanocrystals, (B) physical mixture, (C) poloxamer 407 and (D) MLX raw material.

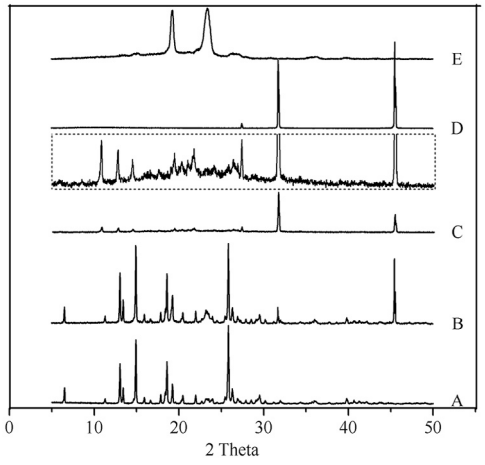

Fig. 7 – PXRD patterns of (A) MLX raw material, (B) physical mixture, (C) nanocrystals, (D) NaCl, and (E) poloxamer 407. Inset: partial enlargement of PXRD patterns of nanocrystals.

Combined the DSC and PXRD results, crystalline status of MLX nanocrystals can be confirmed, although the crystallinity upon nanosizing process was reduced.

3.6. *In vitro transdermal permeation*

In vitro transdermal permeation curves were drawn to compare the drug permeability among the three MLX formulations (Fig. 8). The skin permeation parameters, including J_{ss} and Q_T , are listed in Table 1. A steady increase of MLX permeated through the skin is observed for all formulations. The permeation curves show approximate zero-order kinetics, presenting passive diffusion characteristics. However, the permeated amount of MLX across the skin from nanocrystals increases sharply compared with that from the solution and the suspension. As shown in Table 1, the highest J_{ss} was obtained from nanocrystals, which is 3.15-fold and 3.61-fold higher than the solution and the suspension, respectively. Theoretically, MLX

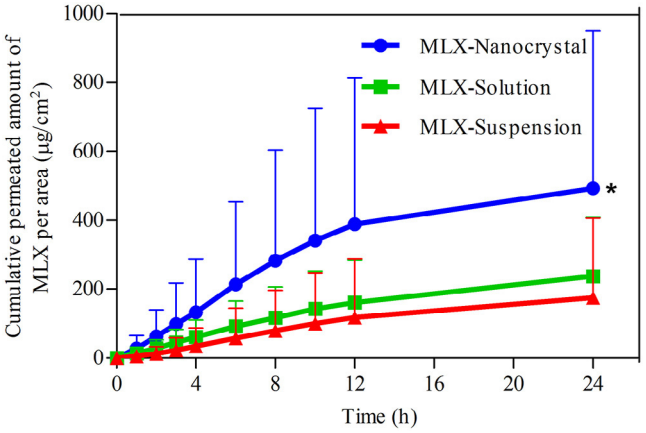

Fig. 8 – *In vitro* skin permeation profiles of MLX from nanocrystals, solution and suspensions. *, $P < 0.05$.

Table 1 – Steady state flux (J_{ss}) and drug deposition per unit skin area (Q_T) for MLX nanocrystals, solution and suspensions ($n = 6$).

	Nanocrystals	Solution	Suspension
J_{ss} (μg/cm²/h)	37.29 ± 39.23	11.83 ± 11.60	10.34 ± 14.92
Q_T (μg/cm)	2.89 ± 1.12	2.36 ± 0.98	4.07 ± 2.07

solution should provide highest transdermal permeation due to the highest concentration gradient. However, the pH of the solution was adjusted to alkalescence to dissolve MLX, leading to ionization of MLX. It is generally accepted that the ionized molecules are far inferior in transdermal permeation than the free ones [28]. The dissociation equilibrium of MLX in the solution decreases the actual concentration gradient of free MLX for transdermal transportation, leading to decreased transdermal driving forces. Nanocrystals increased the apparent solubility and dissolution of MLX [23], providing a high concentration gradient for transdermal permeation. In addition, nanocrystals facilitate penetration into the hair follicles than the solution [29–31]. Since the lower follicular orifice is lacking of stratum corneum barrier, the hair follicle provides a permeable site compared with the skin surfaces [32]. The increased transdermal concentration gradient together with the decreased permeation resistance contributes to the higher J_{ss} of MLX nanocrystals than that of the solution. Nonetheless, it should be noted that both the two preparations show similar Q_T . Q_T was measured at the end of the *in vitro* transdermal permeation experiment, when both preparations have enough contact with the skin and reach the steady transdermal permeation. The measured Q_T is actually the solubility of MLX in the skin. Thus the two preparations show similar Q_T .

However, although the transdermal permeation from suspensions is poor, they provided the highest Q_T among the three formulations (Table 1). This is ascribed to the accumulation of MLX crystals in the hair follicles. However, being different to the nanocrystals, the accumulated MLX crystals cannot be dissolved quickly due to the poor solubility. Although tape stripping was performed to remove crystals that adhere on the skin surface prior to the extraction of residual MLX, the

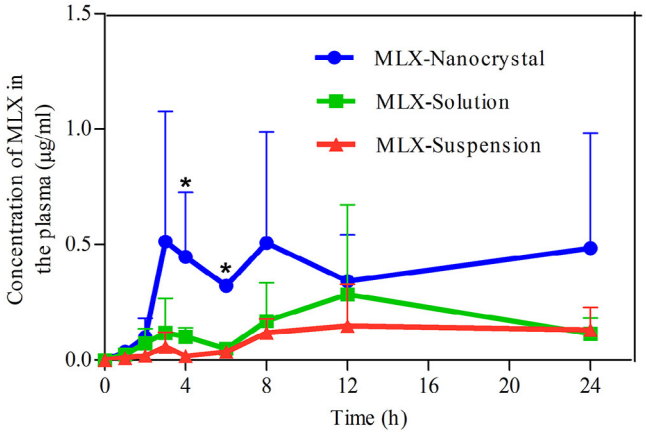

Fig. 9 – Plasma concentration versus time profiles of MLX post dermal administration of MLX nanocrystals, solution and suspensions. *, $P < 0.05$.

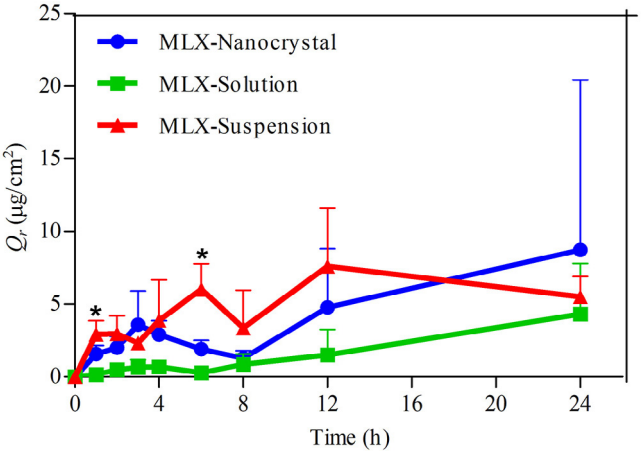

Fig. 10 – Dermal retention per unit skin area (Q_r) versus time profiles of MLX post dermal administration of MLX nanocrystals, solution and suspensions. *, $P < 0.05$.

Table 2 – Primary pharmacokinetic parameters post dermal administration of MLX nanocrystals, solution and suspensions ($n = 6$).

	Nanocrystals	Solution	Suspension
C_{max} (μg/ml)	0.51 ± 0.56	0.28 ± 0.39	0.15 ± 1.18
T_{max} (h)	3.67 ± 0.58	9.33 ± 2.31	10.67 ± 2.31
$AUC_{0\to24h}$ (μg·h/ml)	8.89 ± 4.02	3.45 ± 2.07	2.20 ± 0.42

accumulated crystals inside the hair follicles may not be removed. Then the follicular accumulated MLX crystals plus dissolved MLX molecules in the skin lead to the highest Q_r . However, it should be noted that the residual MLX crystals in the hair follicles may not produce therapeutic effects until they are dissolved and entered into the skin.

3.7. *In vivo transdermal delivery*

Fig. 9 shows the plasma MLX concentration against time post dermal administration of the three formulations. The results are similar to that obtained in the *in vitro* transdermal permeation. The $AUC_{0\to24h}$ of nanocrystals is 2.58- and 4.4-fold that of solution and suspension, respectively (Table 2). Nanocrystals show highest drug concentration in the plasma against time, the plasma MLX concentrations in the first 2 h post administration are similar between nanocrystals and the solution. However, starting from 2 h post administration, the plasma MLX concentration is increased from nanocrystals, compared with that from either the solution or the suspensions, and reaches maximum (C_{max} , 0.51 ± 0.56 μg/ml) around 3 h. Then, the plasma MLX concentration from nanocrystals fluctuates between 0.3 and 0.5 μg/ml, indicating an equilibrium between absorption and metabolism. The prolonged duration of high plasma concentration is advantageous for therapeutic effects, which is ascribed to the maintenance of high transdermal concentration gradient by nanocrystals [33]. On the contrary, the plasma MLX concentration from the solution presents tendency of first rise then descent with C_{max} of 0.28 ± 0.39 μg/ml around 9 h (Fig. 9, Table 2). Due to the poor transdermal permeation, the plasma MLX concentration from suspensions is remained in a low level around 0.15 μg/ml. However, the slow dissolving but continuous permeating of accumulated MLX nanocrystals in hair follicles results in the comparatively steady plasma concentration.

MLX residual in the skin during transdermal permeation is shown in Fig. 10 . Since MLX passively permeated across the skin as indicated by *in vitro* transdermal permeation, Q_r from MLX solution is increased linearly with time. On the contrary, Q_r from both nanocrystals and suspensions fluctuate with time. Due to the facilitated follicular penetration, nanocrystals reach a peak of Q_r around 3 h post administration, then Q_r declined to valley around 8 h. Although nanocrystals facilitate transdermal permeation of MLX, it takes time for MLX molecules to penetrate the skin. Therefore, Q_r from nanocrystals was increased at initial 3 h post administration, which is in accordance with the increment of the plasma MLX concentration. Then Q_r was decreased as more MLX entered into the blood circulation. However, Q_r from nanocrystals was increased again from 8 h post administration, which may be ascribed to the accumulation of MLX nanocrystals inside the hair follicles. Similar to the *in vitro* skin permeation, the suspensions show Q_r higher than the other two formulations due to the accumulation of crystals inside the hair follicles. Nonetheless, the accumulated large crystals cannot be efficiently dissolved in this site, providing low but constant concentration gradient [34]. The low and steady plasma MLX concentration from the suspensions is a good evidence for this inference.

4. Conclusion

MLX nanocrystals can be prepared by nanoprecipitation technique based on acid-base neutralization. Reduced crystallinity of MLX was obtained during the nanoprecipitation process. Nanocrystals increased both *in vitro* and *in vivo* transdermal permeation of MLX. The enhanced permeation may be ascribed to the improved apparent solubility and dissolution

of MLX as well as the accumulation in the hair follicles by nanocrystals. Nanocrystal is a potent formulation to enhance transdermal delivery of MLX.

Conflicts of interest

The authors declare that there are no conflicts of interest.

Acknowledgments

This study was financially supported by Natural Science Foundation of Shanghai (16ZR1403500).

REFERENCES

[1] Ahad A, Raish M, Al-Mohizea AM, et al. Enhanced anti-inflammatory activity of carbopol loaded meloxicam nanoethosomes gel. Int J Biol Macromol 2014;67:99–104.
[2] Lu Y, Zhang X, Lai J, et al. Physical characterization of meloxicam-β-cyclodextrin inclusion complex pellets prepared by a fluid-bed coating method. Particuology 2009;7:1–8.
[3] Alomrani AH, Badran MM. Flexosomes for transdermal delivery of meloxicam: characterization and antiinflammatory activity. Artif Cells Nanomed Biotechnol 2017;45:305–12.
[4] Ah YC, Choi JK, Choi YK, et al. A novel transdermal patch incorporating meloxicam: *in vitro* and *in vivo* characterization. Int J Pharm 2010;385:12–19.
[5] Duangjit S, Obata Y, Sano H, et al. Comparative study of novel ultradeformable liposomes: menthosomes, transfersomes and liposomes for enhancing skin permeation of meloxicam. Biol Pharm Bull 2014;37:239–47.
[6] Yuan Y, Li SM, Mo FK, et al. Investigation of microemulsion system for transdermal delivery of meloxicam. Int J Pharm 2006;321:117–23.
[7] Pawar VK, Singh Y, Meher JG, et al. Engineered nanocrystal technology: in-vivo fate, targeting and applications in drug delivery. J Control Release 2014;183:51–66.
[8] Lu Y, Li Y, Wu W. Injected nanocrystals for targeted drug delivery. Acta Pharm Sin B 2016;6:106–13.
[9] Lu Y, Chen Y, Gemeinhart RA, et al. Developing nanocrystals for cancer treatment. Nanomedicine (Lond) 2015;10:2537–52.
[10] Lu Y, Qi J, Dong X, et al. The *in vivo* fate of nanocrystals. Drug Discov Today 2017;22:744–50.
[11] Sinico C, Pireddu R, Pini E, et al. Enhancing topical delivery of resveratrol through a nanosizing approach. Planta Med 2017. doi:10.1055/s-0042-103688.
[12] Pireddu R, Sinico C, Ennas G, et al. Novel nanosized formulations of two diclofenac acid polymorphs to improve topical bioavailability. Eur J Pharm Sci 2015;77:208–15.
[13] Romero GB, Arntjen A, Keck CM, et al. Amorphous cyclosporin A nanoparticles for enhanced dermal bioavailability. Int J Pharm 2016;498:217–24.
[14] Xu Y, Liu X, Lian R, et al. Enhanced dissolution and oral bioavailability of aripiprazole nanosuspensions prepared by nanoprecipitation/homogenization based on acid-base neutralization. Int J Pharm 2012;438:287–95.
[15] Chen H, Wan J, Wang Y, et al. A facile nanoaggregation strategy for oral delivery of hydrophobic drugs by utilizing acid-base neutralization reactions. Nanotechnology 2008;19:375104.
[16] Xie Y, Chen Z, Su R, et al. Preparation and optimization of amorphous ursodeoxycholic acid nanosuspensions by nanoprecipitation based on acid-base neutralization for enhanced dissolution. Curr Drug Deliv 2017;14:483–91.
[17] Jantharaprapap R, Stagni G. Effects of penetration enhancers on *in vitro* permeability of meloxicam gels. Int J Pharm 2007;343:26–33.
[18] Khurana S, Jain NK, Bedi PM. Development and characterization of a novel controlled release drug delivery system based on nanostructured lipid carriers gel for meloxicam. Life Sci 2013;93:763–72.
[19] Khurana S, Jain NK, Bedi PM. Nanoemulsion based gel for transdermal delivery of meloxicam: physico-chemical, mechanistic investigation. Life Sci 2013;92:383–92.
[20] Ren Q, Deng C, Meng L, et al. *In vitro*, *ex vivo*, and *in vivo* evaluation of the effect of saturated fat acid chain length on the transdermal behavior of ibuprofen-loaded microemulsions. J Pharm Sci 2014;103:1680–91.
[21] Kim JH, Ko JA, Kim JT, et al. Preparation of a capsaicin-loaded nanoemulsion for improving skin penetration. J Agric Food Chem 2014;62:725–32.
[22] Bae JW, Kim MJ, Jang CG, et al. Determination of meloxicam in human plasma using a HPLC method with UV detection and its application to a pharmacokinetic study. J Chromatogr B Analyt Technol Biomed Life Sci 2007;859:69–73.
[23] Ochi M, Kawachi T, Toita E, et al. Development of nanocrystal formulation of meloxicam with improved dissolution and pharmacokinetic behaviors. Int J Pharm 2014;474:151–6.
[24] Demiralay EC, Alsancak G, Ozkan SA. Determination of pKa values of nonsteroidal antiinflammatory drug-oxicams by RP-HPLC and their analysis in pharmaceutical dosage forms. J Sep Sci 2009;32:2928–36.
[25] Van Eerdenbrugh B, Van den Mooter G, Augustijns P. Top-down production of drug nanocrystals: nanosuspension stabilization, miniaturization and transformation into solid products. Int J Pharm 2008;364:64–75.
[26] Teixeira RS, Cova TFGG, Silva SMC, et al. Novel serine-based gemini surfactants as chemical permeation enhancers of local anesthetics: a comprehensive study on structure–activity relationships, molecular dynamics and dermal delivery. Eur J Pharm Biopharm 2015;93:205–13.
[27] Freag MS, Elnaggar YS, Abdallah OY. Development of novel polymer-stabilized diosmin nanosuspensions: *in vitro* appraisal and *in vivo* permeation. Int J Pharm 2013;454:462–71.
[28] Delgado-Charro MB, Guy RH. Effective use of transdermal drug delivery in children. Adv Drug Deliv Rev 2014;73:63–82.
[29] Lademann J, Richter H, Teichmann A, et al. Nanoparticles–an efficient carrier for drug delivery into the hair follicles. Eur J Pharm Biopharm 2007;66:159–64.
[30] Patzelt A, Richter H, Knorr F, et al. Selective follicular targeting by modification of the particle sizes. J Control Release 2011;150:45–8.
[31] Zhai X, Lademann J, Keck CM, et al. Nanocrystals of medium soluble actives–novel concept for improved dermal delivery and production strategy. Int J Pharm 2014;470:141–50.
[32] Mittal A, Raber AS, Lehr CM, et al. Particle based vaccine formulations for transcutaneous immunization. Hum Vaccin Immunother 2013;9:1950–5.
[33] Vidlářová L, Romero GB, Hanuš J, et al. Nanocrystals for dermal penetration enhancement – effect of concentration and underlying mechanisms using curcumin as model. Eur J Pharm Biopharm 2016;104:216–25.
[34] Romero GB, Chen R, Keck CM, et al. Industrial concentrates of dermal hesperidin smartCrystals®–production, characterization & long-term stability. Int J Pharm 2015;482:54–60.